

COBEM-2017-1445

AERODYNAMIC STUDY OF FORMULA 1 WING IN GROUND EFFECT USING COMPUTATIONAL FLUID DYNAMICS

Igor Carvalho Santos de Oliveira

Luis Felipe de Aguilar Paulinyi

Universidade de Brasília - Faculdade de Tecnologia, Campus Universitário Darcy Ribeiro, Brasília - CEP 70910-900

igorcso93@gmail.com

paulinyi@unb.com.br

Abstract. A study of a Formula 1 wing in ground effect using CFD tools in order to establish guidelines for an accurate numerical approach on this type of flow simulation comparing various types of turbulence models and mesh models provided by commercial CFD package Star-CCM+. The work focuses specifically on RANS simulations of the F1 Tyrrel 026 front wing for which experimental work has been conducted at the University of Southampton's moving belt wind tunnel. Spalart-Allmaras and $k-\varepsilon$ turbulence models are evaluated as well as dodecahedral, hexahedral and tetrahedral element mesh models. The coefficients of lift and drag are plotted against the height/cord ratio and compared with the experimental results. The pressure coefficient distribution, wake velocity profile and boundary layer profile are also compared. The flow structures were evaluated with respect to the ones observed by PIV techniques in the experiment. The lift coefficient was well predicted but drag showed divergence for higher ground clearances. The simulation was able to reproduce the experiment's flow structures such as the Venturi effect, tip vortex and the increase of separated flow with the wing closer to the ground. The simulation was also able to reproduce the downforce reduction phenomenon.

Keywords: Motorsport Engineering, CFD, Turbulence Models, Ground Effect, Downforce

1. INTRODUCTION

In light of high computational performance equipment becoming more accessible, it is no surprise that the practice of CFD analysis is reaching newer applications and practitioners. However, there are still problems with Direct Numerical Simulations of high Reynolds number turbulent flows, which represent a large portion of applied flow simulation analysis. Regarding this issue, a common approach adopted then is to combine turbulence models in RANS simulated flows with wind tunnel experiments on scaled down prototypes. The experimental part is used for validation and adjustment of the parameters set into the numerical approach. Many industry related applications already have well validated models, however, alternative applications have many opportunities for further study and documentation. This is specially the case for competitive applications such as motorsports. Due to its nature, its common for researches in this area being kept from publication. With this in mind, the purpose of this work is to study the impact of different turbulence models and mesh models in a RANS simulated Formula 1 wing in ground effect for which there is experimental data available and, in this manner, help to establish some guidelines for approaching this kind of problem.

1.1 Background

Wings producing negative lift in ground effect have been studied in detail by Zerihan and Zhang (2000) and Zerihan (2001). In their research, they were able to reproduce the ground effect by installing a moving belt rig and boundary layer suction slots inside the wind tunnel. The investigation was performed on a single element rectangular wing with 1100 mm span and 223,4 mm chord attached with end plates. The profile used was the main element of the Tyrrel 026 Formula 1 front wing. Among other findings, it is highlighted the shape of the ground effect curve. It shows the behaviour of the downforce for a fixed angle of attack with varying heights (Fig. 1).

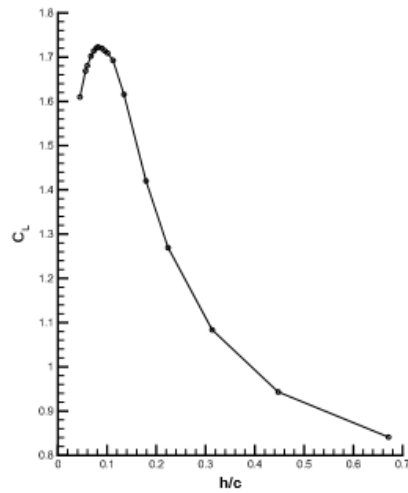


Figure 1. Ground Effect Curve - Zerihan (2001)

As discussed by them, bringing the wing closer to the ground (in the figure, represented by the dimensionless variable h/c , the height to chord ratio), at first increases the lift coefficient (negative lift, in this case). This is due to a Venturi effect, which is an increase in the flow velocity under the wing because of the restriction imposed by the wing being near the ground. This trend eventually reaches a maximum and turns back as the gradual increase of the separated region due to high pressure gradients extend to great distance along the chord.

The work here presented used the same setup as described above for the simulations. The computational procedure is described below and at the end the results are compared to the experimental data of Zhang and Zerihan’s study.

2. COMPUTATIONAL PROCEDURE

The computational procedure was conducted firstly with a domain study and a mesh study for the hexahedral mesh model using Spalart-Allmaras turbulence model. Later, the parameters defined by these studies were set for the other mesh models and turbulence models. The mesh models evaluated were the Polyhedral (dodecahedral element shape), Trimmed (hexahedral element shape) and Tetrahedral (tetrahedral element shape) meshes. The turbulence models evaluated were the $k-\epsilon$ and the Spalart-Allmaras models.

The domain study is shown below (Fig. 2). In it, it is plotted the lift and drag coefficients against the reference number of the domain used on the simulation. From 1 to 4 all 3 dimensions grow according to Table 1 (in terms of the chord distance c). The plot suggests that domain 4 is converged for both C_L and C_D but it was verified that there still was a great instability with the residuals of the simulation for this domain size (Fig. 3). A further increase in it showed that this problem was no longer present (Fig. 3). The dimensions of this 5th domain (Tab. 2) were then set as the standard to study all other parameters. Fig. 4 shows graphically the final result. It is important to notice that these dimensions do not reflect the dimensions of the wind tunnel used in the experiment.

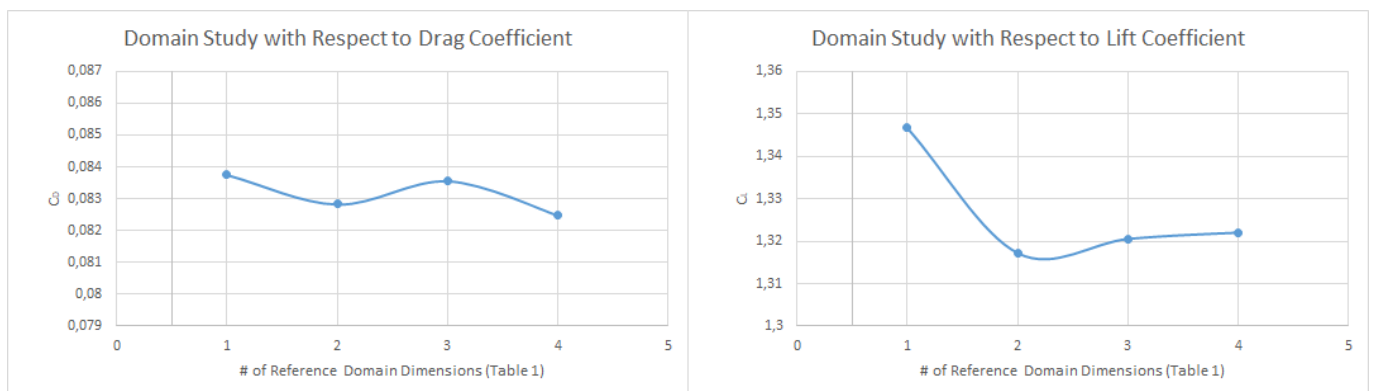


Figure 2. Domain Study

Table 1. Dimensions of Reference Domain

# Reference	Upstream	Downstream	height	Depth
1	8c	10c	8c	10c
2	9c	11c	9c	11c
3	10c	12c	10c	12c
4	11c	13c	11c	13c

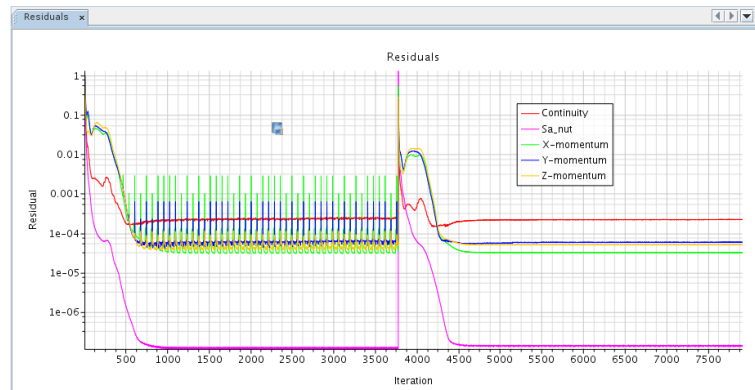


Figure 3. Residuals Convergence

Table 2. Final Domain Dimensions

# Reference	Upstream	Downstream	Height	Depth
5	16c	16c	10c	12c

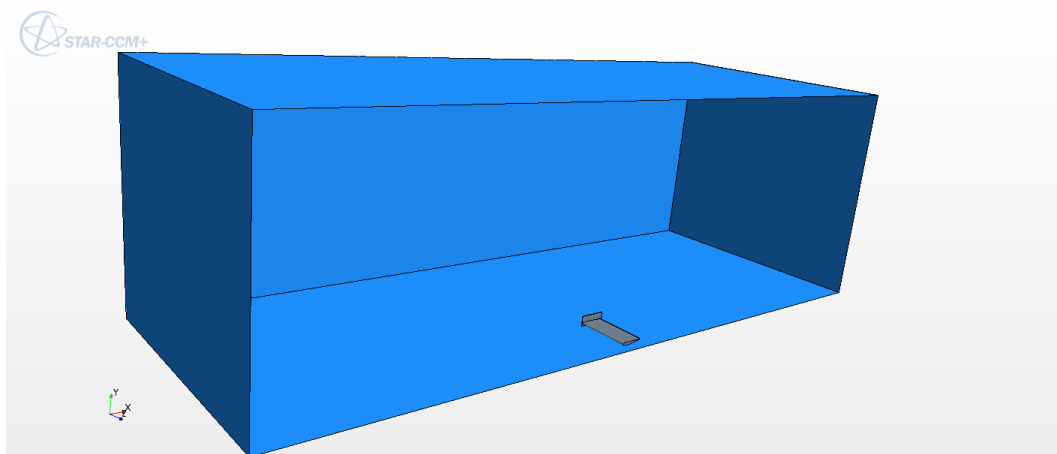


Figure 4. Domain

The mesh refinement independence study was then conducted for both lift and drag coefficients showing that, between 7 million and 8.5 million cells, the variation of lift coefficient was of 0.5% and the drag coefficient variation was 1.7%. At this point it was assumed that the solution was mesh independent and the 8.5 million cells configuration was used.

The definition of the regions of specific refinement are shown in the figures below. As illustrated, three regions were selected for cell size control. Under the wing (Fig. 5, 5% base size), due to high gradients, and also in the wake (not shown here, 10% base size) and wing tip vortex region (Fig. 6, 10% base size).

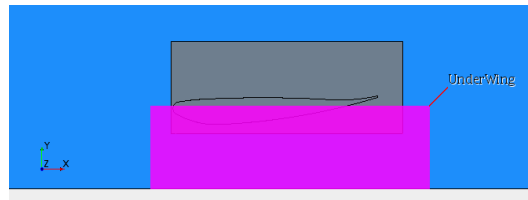


Figure 5. *Cell Refinement Control Region Under the Wing Set to 5% Base Size*

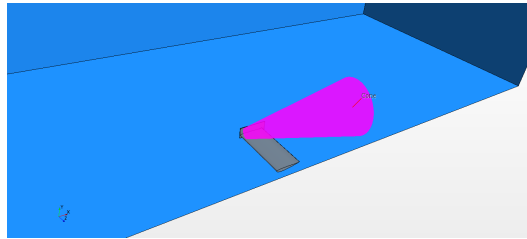


Figure 6. *Cell Refinement Control at Tip Vortex Region Set to 10% Base Size*

The tetrahedral and dodecahedral mesh models showed problems with this approach. Because of the abrupt cell size change in and out of this region (Fig. 7), it was decided to use a rectangular volume enveloping the wing to set the specific cell refinement for both these models.

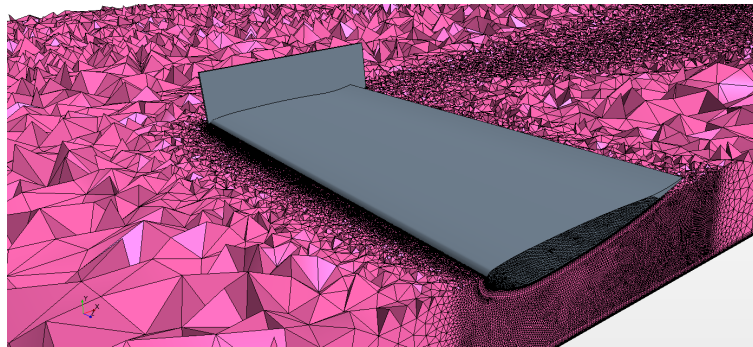


Figure 7. *Poor Quality Tetrahedral Mesh*

The physics models and mesh parameters were defined in the following manner.

Boundary conditions chosen:

- Inlet - Velocity inlet of 30 m/s in the x direction
- Outlet - Zero pressure gradient
- Wing - No-slip condition
- Symmetry Plane - Symmetry condition
- Ground - No-slip condition and 30 m/s velocity in the x direction
- Side and top boundaries - Symmetry condition

Physics models chosen:

- All y^+ wall treatment
- Constant Density

- Gas
- Gradients
- RANS
- Segregated Flow
- SA turbulence model
- Standard SA
- Steady
- Three dimensional
- Turbulent

Other mesh parameters:

Table 3. Mesh Parameters

Base size	0,06 m
Target Surface Size	100%
Minimum Surface Size	10%
Surface Curvature	100
Surface Growth Rate	1,3
Number of Prism Layers	20
Prism Layer Stretching	1,3
Prism Layer Total Thickness	7 mm
Volume Growth Rate	Very Slow
Maximum Cell Size	500%

3. RESULTS

At a fixed angle of attack of $\alpha = 3.45^\circ$ (or 1° as set by Zhang's redefined zero reference), the wing was simulated at different heights above the ground. Figures 8 and 9 show the performance of the different models against the experimental data. It is important to say that this comparison was made using the values of the wing with fixed boundary layer transitioners. As the simulated boundary layer already begins turbulent, it was decided that this approach resulted in a more coherent comparison.

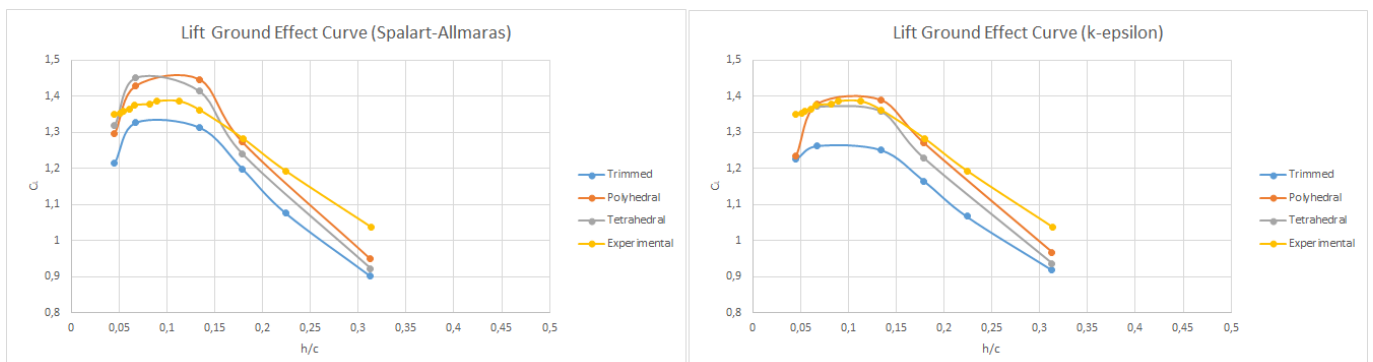


Figure 8. Lift Coefficient Plotted Against Ground Height

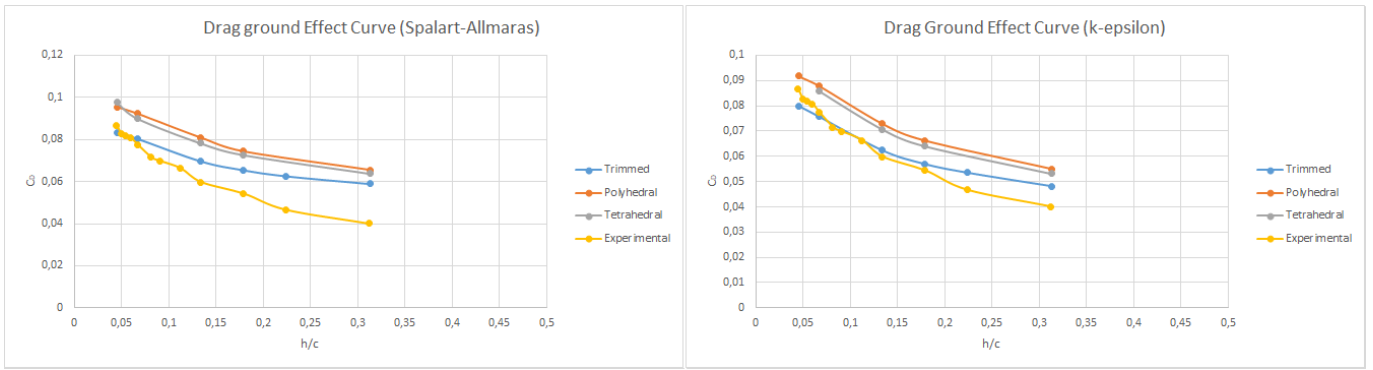


Figure 9. Drag Coefficient Plotted Against Ground Height

The venturi effect and gradual growth of the separation region were also predicted by the simulation as shown in Fig. 10. In red, the intensification of the flow velocity below the wing, showing that there is a lower pressure field contributing to the downforce. The dark blue area shows stagnated flow, which are separated boundary layer recirculation regions at the trailing edge.

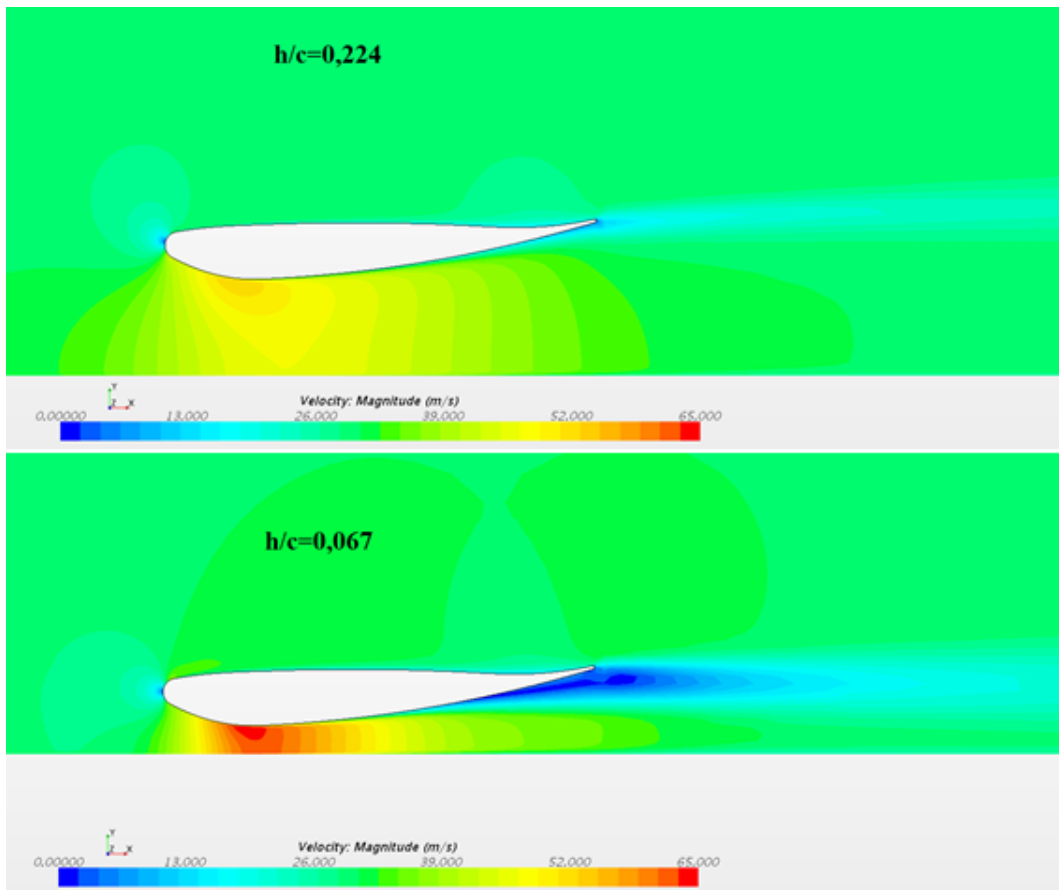


Figure 10. Venturi Effect and Separation Growth

Wing tip vortex intensification and decay are also reproduced by the simulations. Also referred to as Edge Vortex (Zhang *et al.* (2006)) for being formed at the edge of the end plate, it can be seen in Fig. 11 and 12 that it follows the same trend as the result obtained from Particle Image Velocimetry experimentally. One can see that the units between the two figures are different. This is due to the fact that the software does not provide the dimensionless vorticity plot. Regardless, the limits of the plot generated by the simulation were set as to reflect the same values as dimensionless unit used to present the experimental data.

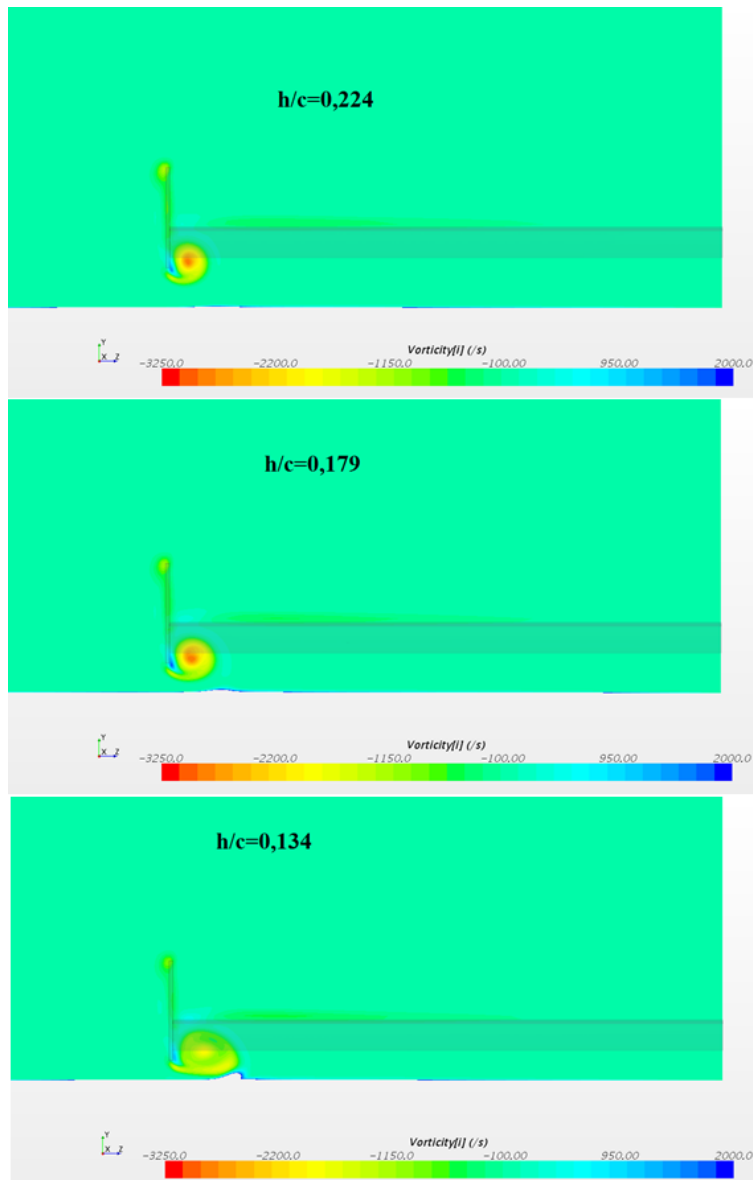


Figure 11. *Vorticity Plot Obtained From the Simulations*

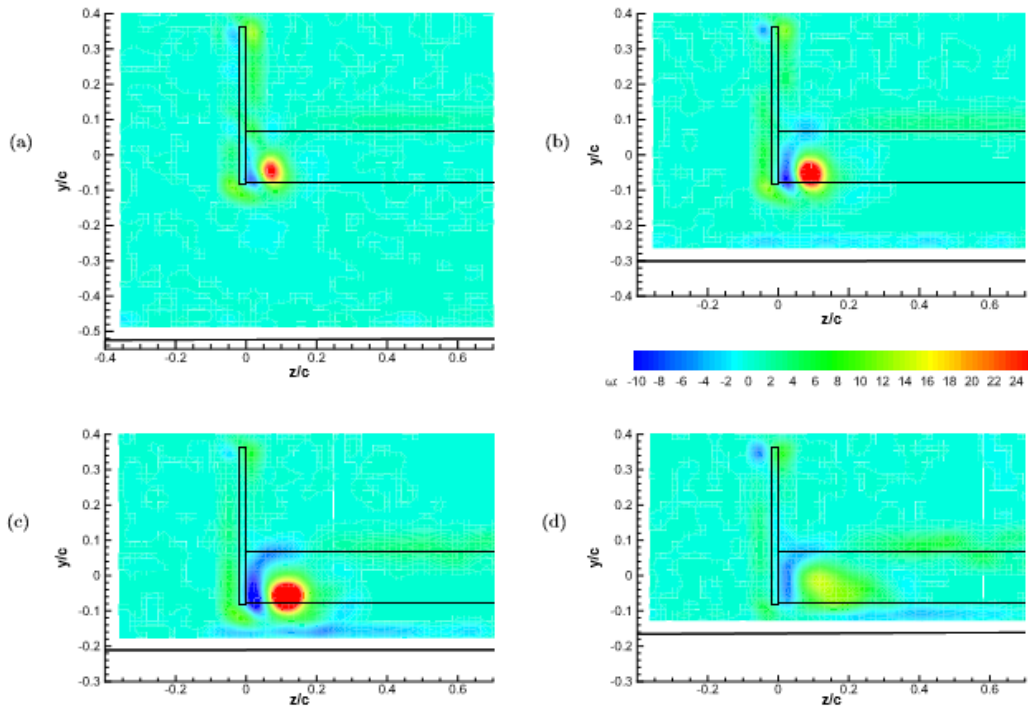


Figure 12. Vorticity Plot Obtained From the PIV Analysis on the Experiment

A study comparing pressure distribution, wake velocity profile and boundary layer profile was also conducted as shown below (Figures 13, 14, 15, 16 and 17):

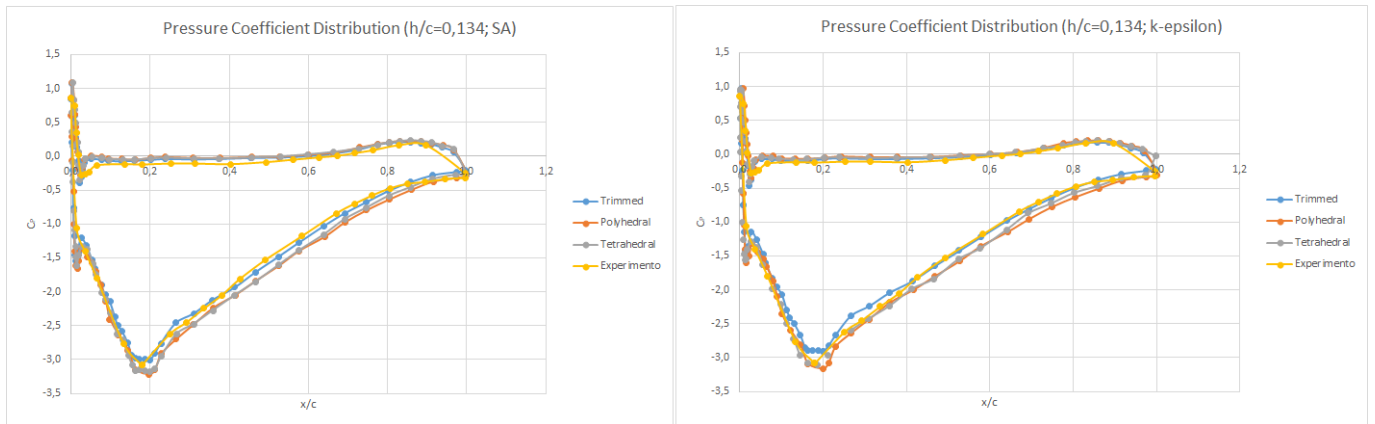


Figure 13. Comparison of Pressure Coefficient Distribution Along the Center Chord

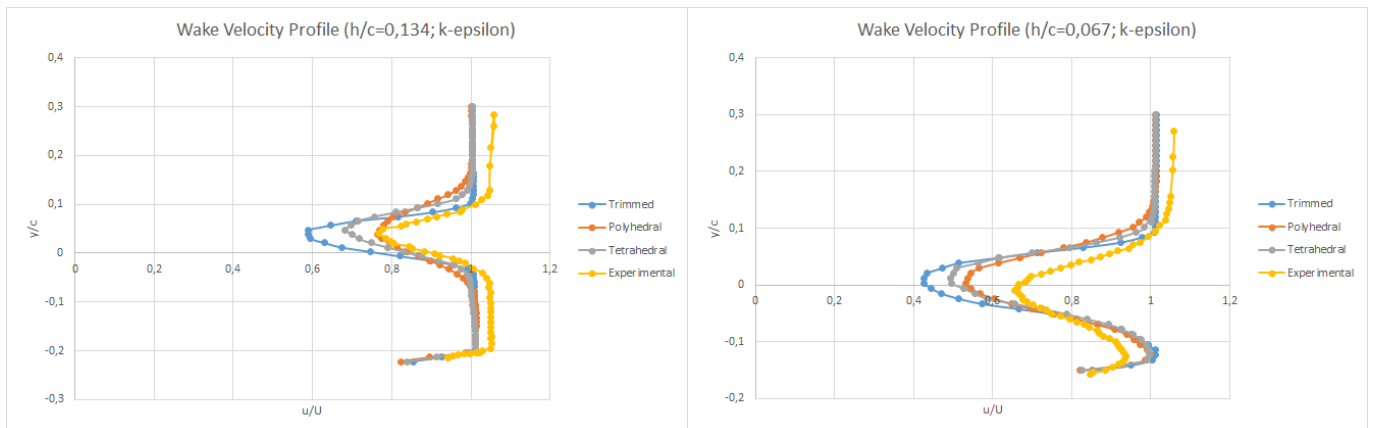


Figure 14. Comparison of Wake Velocity Profile with K-Epsilon Turbulence Model

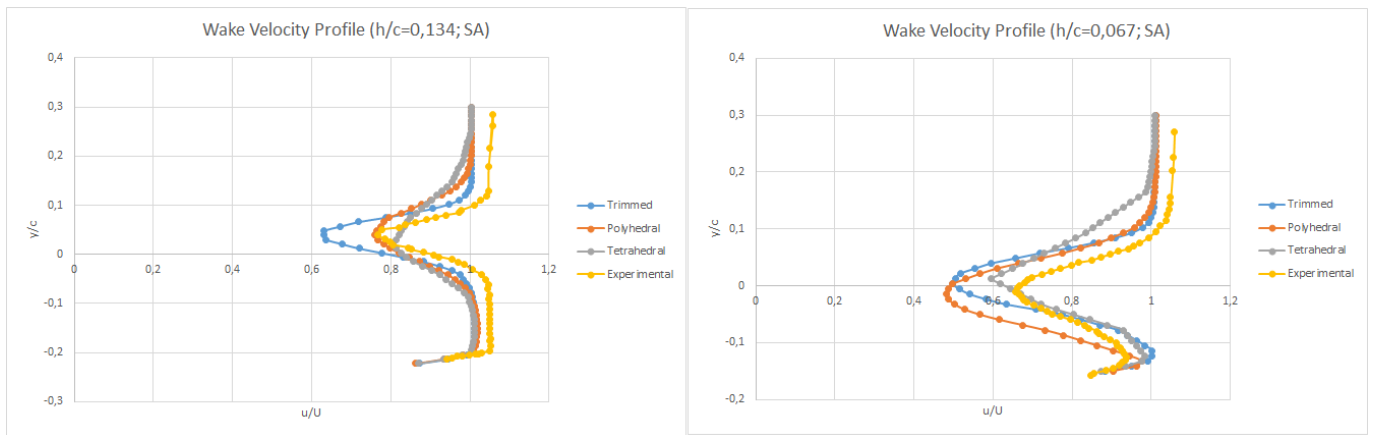


Figure 15. Comparison of Wake Velocity Profile with Spalart-Allmaras Turbulence Model

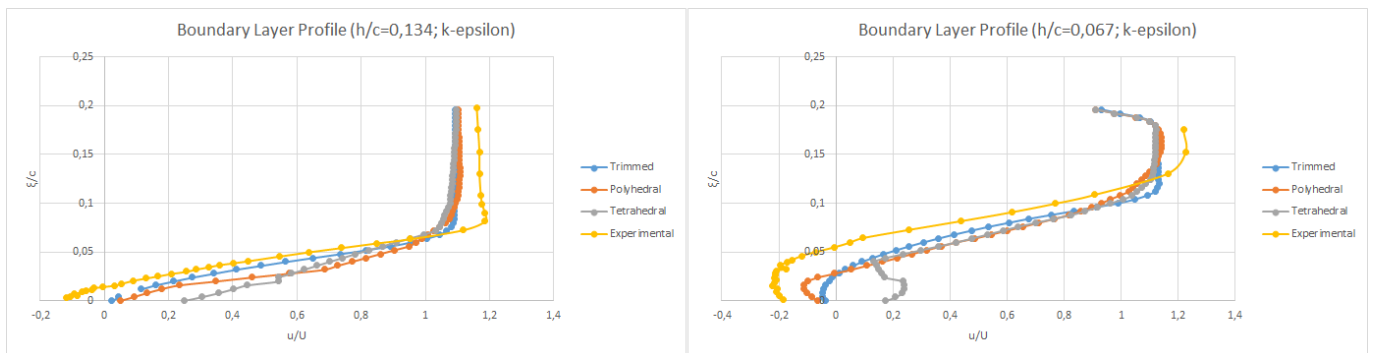


Figure 16. Comparison of Boundary Layer Profile with K-Epsilon Turbulence Model

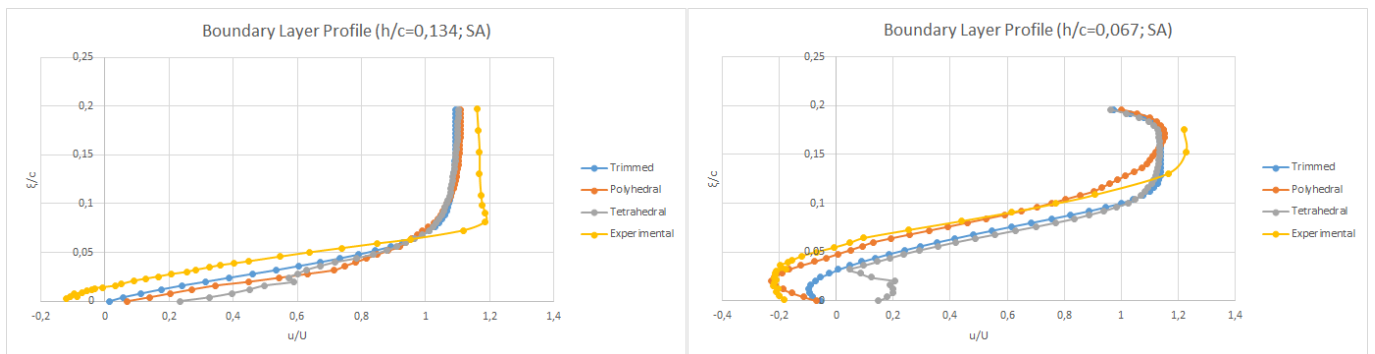


Figure 17. Comparison of Boundary Layer Profile with Spalart-Allmaras Turbulence Model

Even though the Tetrahedral mesh model showed diverging behaviour with respect to boundary layer profile, the mesh didn't seem to have a problem (Fig. 18).

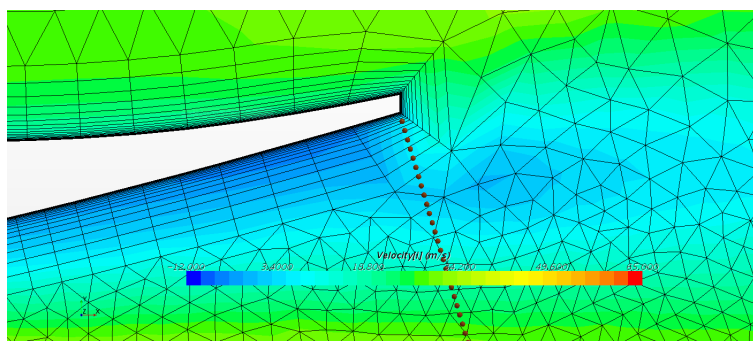


Figure 18. Tetrahedral Mesh Detail

4. CONCLUSIONS

Each combination of models seem to work well in different aspects. It is relevant to highlight the $k-\varepsilon$ turbulence model's performance in capturing with best precision values of drag coefficient, the dodecahedral mesh model in capturing the wake and boundary layer profiles and the tetrahedral mesh, combined with k -epsilon turbulence model, in predicting the lift coefficient.

Also notable, the drag curves were all overestimated. It is believed that this might be linked to the RANS weak performance in capturing the effects of high shear and separated regions because of the transient nature of these. The underestimated wake velocity profile obtained by all of the simulations might be understood as a reflection of this higher drag prediction. As the conservation of momentum is one of the governing equations, the higher drag generated impacts the velocity profile at the wake.

The pressure distribution along the central chord was very precise in comparison to the experimental results. It is possible that differences in prediction of the tip vortex might be altering the distribution along the wing span, causing the overall C_L and C_D to be different even though the central chord pressure distribution is very similar. Friction drag might also play a role in this discrepancy. Unfortunately, for the case of fixed boundary layer transitioners, the experiment does not provide pressure coefficient distributions along the wing span nor does it provide segregated friction drag values.

5. REFERENCES

- Zerihan, J., 2001. *An investigation into the aerodynamics of wings in ground effect*. Ph.D. thesis, University of Southampton.
- Zerihan, J. and Zhang, X., 2000. "Aerodynamics of a single element wing in ground effect". *Journal of aircraft*, Vol. 37, No. 6, pp. 1058–1064.
- Zhang, X., Toet, W. and Zerihan, J., 2006. "Ground effect aerodynamics of race cars". *Applied Mechanics Reviews*, Vol. 59, No. 1, pp. 33–49.

6. RESPONSIBILITY NOTICE

The authors are the only responsible for the printed material included in this paper.